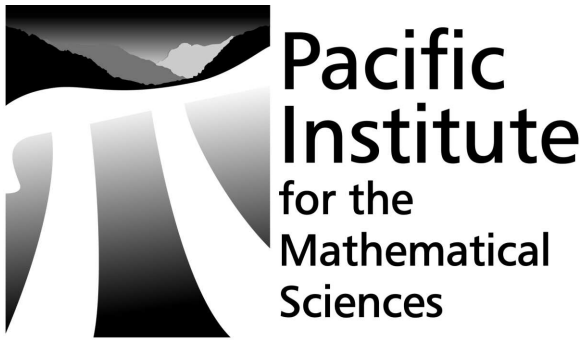

Energy Norm A Posteriori Error Estimation for Mixed Discontinuous Galerkin Approximations of the Stokes Problem

Paul Houston
Department of Mathematics
University of Leicester
Leicester, United Kingdom

Dominik Schötzau
Mathematics Department
University of British Columbia
Vancouver, BC, Canada

Thomas P. Wihler
School of Mathematics
University of Minnesota
Minneapolis, MN, USA

Preprint number: PIMS-04-4
Received on January 23, 2004

Energy Norm A Posteriori Error Estimation for Mixed Discontinuous Galerkin Approximations of the Stokes Problem

Paul Houston (paul.houston@mcs.le.ac.uk) *
Department of Mathematics, University of Leicester, Leicester LE1 7RH, UK

Dominik Schötzau (schoetzau@math.ubc.ca)
Mathematics Department, University of British Columbia, 1984 Mathematics Road, Vancouver, BC V6T 1Z2, Canada

Thomas P. Wihler (wihler@math.umn.edu) †
School of Mathematics, University of Minnesota, 206 Church Street SE, Minneapolis, MN 55455, USA

Abstract. In this paper, we develop the a posteriori error estimation of mixed discontinuous Galerkin finite element approximations of the Stokes problem. In particular, we derive computable upper bounds on the error, measured in terms of a natural (mesh–dependent) energy norm. This is done by rewriting the underlying method in a non-consistent form using appropriate lifting operators, and by employing a decomposition result for the discontinuous spaces. A series of numerical experiments highlighting the performance of the proposed a posteriori error estimator on adaptively refined meshes are presented.

Keywords: Discontinuous Galerkin methods, A posteriori error estimation, Stokes problem

1. Introduction

In recent years, several authors have been concerned with the development of mixed discontinuous Galerkin (DG, for short) methods for the numerical approximation of incompressible fluid flow problems. We first mention here the work of Baker, Jureidini and Karakashian [2] and Karakashian and Jureidini [16] who studied piecewise solenoidal discontinuous Galerkin methods for the Stokes and Navier-Stokes equations. Later, Cockburn, Kanschat, Schötzau and Schwab [7] and Cockburn, Kanschat and Schötzau [6] proposed and analyzed local discontinuous Galerkin discretizations for Stokes and Oseen flow. Hansbo and Larson [12], Toselli [22] and Girault, Rivière and Wheeler [11] employed mixed interior penalty methods for the approximation of saddle point problems arising in linear elasticity and fluid flow. Finally, the papers

* Funded by the EPSRC (Grant GR/R76615).
† Funded by the Swiss National Science Foundation (Grant PBEZ2-102321).

of Toselli [22], Schötzau, Schwab and Toselli [20], and Schötzau and Wihler [21] have been devoted to the extension of mixed DG methods from the h– to the hp-version of the finite element method. The key advantages of discontinuous Galerkin approaches in comparison with standard conforming finite element methods lie in their robustness and stability in transport-dominated regimes, their flexibility in the mesh-design, and their freedom in the choice of velocity-pressure spaces.

While an extensive body of literature is available with a priori error analyses for discontinuous Galerkin discretizations applied to elliptic problems, there are considerably fewer papers that are concerned with a posteriori error estimation for such approaches. In the context of energy norm error estimation, we mention here the recent papers by Becker, Hansbo and Larson [3], Becker, Hansbo and Stenberg [4] and Karakashian and Pascal [17], which consider diffusion problems, as well as the article by Houston, Perugia and Schötzau [14], where computable upper bounds on the energy norm of the error in the mixed DG approximation to the time–harmonic Maxwell operator were established. For L^2-norm or functional error estimation for DG discretizations of elliptic problems, we refer to Becker, Hansbo and Stenberg [4], Kanschat and Rannacher [15], Rivière and Wheeler [19] and the references therein.

In this paper, we initiate the development of the a posteriori error estimation and adaptive mesh design for mixed discontinuous Galerkin approximations of the Stokes problem for incompressible fluid flow. In particular, computable upper bounds on the error, measured in terms of a natural (mesh–dependent) DG energy norm, will be derived. In contrast to the approach of Becker, Hansbo and Larson [3] and Houston, Perugia and Schötzau [14], which is based on employing a suitable Helmholtz decomposition of the error, together with the underlying conservation properties of DG methods, or the approach of Becker, Hansbo and Stenberg [4], which hinges on a saturation assumption on the meshes, here we present a new technique to derive a posteriori error bounds. Indeed, the analysis presented in this article is based on rewriting the method in a non-consistent manner using lifting operators in the spirit of Arnold, Brezzi, Cockburn and Marini [1] (see also Perugia and Schötzau [18] and Schötzau, Schwab and Toselli [20]), and employing the decomposition result for discontinuous spaces from Houston, Perugia and Schötzau [13]; the proof of this result is based on a crucial approximation property from Karakashian and Pascal [17, Section 2]. The performance of the proposed error bound within an adaptive mesh refinement procedure will be demonstrated for two-dimensional problems with both smooth and singular analytical solutions. In particular, the results show that the error estimator converges to zero at the same

asymptotic rate as the energy norm of the actual error on a sequence of non-uniform adaptively refined meshes.

The outline of the paper is as follows. In Section 2, we introduce a mixed discontinuous Galerkin method for the Stokes problem. In Section 3, our a posteriori error bound is presented and discussed. The derivation of this result can be found in Section 4. In Section 5, we present a series of numerical experiments to highlight the performance of the proposed error estimator within an automatic mesh refinement algorithm. Finally, in Section 6 we summarize the work presented in this paper and draw some conclusions.

2. Mixed DG Approximation of Stokes Flow

In this section, we introduce a mixed discontinuous Galerkin finite element method for the discretization of the Stokes problem.

2.1. Function Spaces

We begin by defining the function spaces that will be used throughout the paper. Given a bounded domain D in $\mathbb{R}^d$, $d = 2, 3$, we write $H^t(D)$ to denote the usual Sobolev space of real-valued functions with norm $\|\cdot\|_{t,D}$, $t \geq 0$. In the case $t = 0$, we set $L^2(D) = H^0(D)$. We define $H_0^1(D)$ to be the subspace of functions in $H^1(D)$ with zero trace on ∂D. In addition, we set $L_0^2(D) = \{q \in L^2(D) : \int_D q\, d\mathbf{x} = 0\}$. For a function space $X(D)$, let $X(D)^d$ and $X(D)^{d\times d}$ denote the spaces of vector and tensor fields whose components belong to $X(D)$, respectively. These spaces are equipped with the usual product norms which, for simplicity, are denoted in the same way as the norm in $X(D)$. If Λ is a subset of ∂D, we use $\|\cdot\|_{0,\Lambda}$ to denote the L^2-norm in $L^2(\Lambda)$, $L^2(\Lambda)^d$ and $L^2(\Lambda)^{d\times d}$. For vectors $\mathbf{v}, \mathbf{w} \in \mathbb{R}^d$, and matrices $\underline{\sigma}, \underline{\tau} \in \mathbb{R}^{d\times d}$, we define $\nabla\mathbf{v}$ by $(\nabla\mathbf{v})_{ij} = \partial_j v_i$, $\nabla \cdot \underline{\sigma}$ by $(\nabla \cdot \underline{\sigma})_i = \sum_{j=1}^d \partial_j \sigma_{ij}$, and set $\underline{\sigma} : \underline{\tau} = \sum_{i,j=1}^d \sigma_{ij}\tau_{ij}$. We further denote by $\mathbf{v} \otimes \mathbf{w}$ the matrix whose ij-th entry is $v_i\, w_j$. With this notation, we note that $\mathbf{v} \cdot \underline{\sigma} \cdot \mathbf{w} = \sum_{i,j=1}^d v_i \sigma_{ij} w_j = \underline{\sigma} : (\mathbf{v} \otimes \mathbf{w})$.

2.2. The Stokes Problem

Let Ω be a polygonal or polyhedral Lipschitz domain in $\mathbb{R}^d$, $d = 2, 3$, with boundary $\Gamma = \partial\Omega$. Given $\mathbf{f} \in L^2(\Omega)^d$ and $\nu > 0$, we consider the Stokes problem: find the velocity field $\mathbf{u}$ and the pressure p such that

$$-\nu\Delta\mathbf{u} + \nabla p = \mathbf{f} \qquad \text{in } \Omega, \tag{1a}$$

$$\nabla \cdot \mathbf{u} = 0 \qquad \text{in } \Omega, \tag{1b}$$

$$\mathbf{u} = \mathbf{0} \qquad \text{on } \Gamma. \tag{1c}$$

By introducing the forms

$$A(\mathbf{u},\mathbf{v}) = \int_\Omega \nu \nabla \mathbf{u} : \nabla \mathbf{v}\, d\mathbf{x}, \qquad B(\mathbf{v},q) = -\int_\Omega q \nabla \cdot \mathbf{v}\, d\mathbf{x},$$

the standard weak formulation of the Stokes problem (1) reads: find $(\mathbf{u},p) \in H_0^1(\Omega)^d \times L_0^2(\Omega)$ such that

$$\left\{ \begin{array}{rcl} A(\mathbf{u},\mathbf{v}) \;+\; B(\mathbf{v},p) & = & \displaystyle\int_\Omega \mathbf{f}\cdot\mathbf{v}\, d\mathbf{x}, \\ -B(\mathbf{u},q) & = & 0 \end{array} \right.$$

for all $(\mathbf{v},q) \in H_0^1(\Omega)^d \times L_0^2(\Omega)$. Due to the continuous inf-sup condition

$$\inf_{0\neq q\in L_0^2(\Omega)} \sup_{0\neq \mathbf{v}\in H_0^1(\Omega)^d} \frac{-\int_\Omega q\nabla\cdot\mathbf{v}\, d\mathbf{x}}{\|\nabla\mathbf{v}\|_{0,\Omega}\|q\|_{0,\Omega}} \geq \kappa > 0, \tag{2}$$

where κ is the inf-sup constant, depending only on Ω, the variational formulation above is well-posed and has a unique solution $(\mathbf{u},p) \in H_0^1(\Omega)^d \times L_0^2(\Omega)$; see Girault and Raviart [10] or Brezzi and Fortin [5] for details.

The regularity results in Dauge [8] show that, under the foregoing assumptions, the solution $(\mathbf{u},p)$ of the Stokes problem belongs to $H^{1+\varepsilon}(\Omega)^d \times H^\varepsilon(\Omega)$ with a regularity exponent $\varepsilon > 0$. The maximal value of ε only depends on the opening angles at the edges and faces of the domain. In particular, for a convex domain, we have $\varepsilon = 1$.

2.3. Meshes and Traces

Throughout, we assume that the domain Ω can be subdivided into shape-regular affine meshes $\mathcal{T}_h$ consisting of parallelograms $\{K\}$ ($d = 2$) or parallelepipeds $\{K\}$ ($d = 3$). For each $K \in \mathcal{T}_h$, we denote by $\mathbf{n}_K$ the outward unit normal vector on the boundary ∂K, and by h_K the elemental diameter. As usual, we define the mesh size by $h = \max_{K\in\mathcal{T}_h} h_K$.

An interior face of $\mathcal{T}_h$ is the (non-empty) $(d-1)$-dimensional interior of $\partial K^+ \cap \partial K^-$, where K^+ and K^- are two adjacent elements of $\mathcal{T}_h$. Similarly, a boundary face of $\mathcal{T}_h$ is the (non-empty) $(d-1)$-dimensional interior of $F \cap \Gamma$ where F is an entire face of an element K at the boundary. We denote by $\mathcal{F}_\mathcal{I}$ the set of all interior faces, by $\mathcal{F}_\mathcal{D}$ the set of all boundary faces, and define $\mathcal{F} = \mathcal{F}_\mathcal{I} \cup \mathcal{F}_\mathcal{D}$. We allow for so-called 1-irregular meshes, that is, any interior face $F \in \mathcal{F}_\mathcal{I}$ is an entire elemental face of at least one of the two adjacent elements sharing F, and the number of interior faces contained in an elemental face is bounded by $2d-2$. This assumption implies that the local mesh sizes are of

bounded variation, that is, there is a positive constant C, depending only on the shape-regularity of the mesh, such that $Ch_K \leq h_{K'} \leq C^{-1}h_K$, whenever K and K' share a common face.

Next, we define the trace operators that are needed for the DG method. To this end, let K^+ and K^- be two adjacent elements of $\mathcal{T}_h$, and $\mathbf{x}$ an arbitrary point on the interior face $F \in \mathcal{F}_\mathcal{I}$ with $F = \partial K^+ \cap \partial K^-$. Furthermore, let q, $\mathbf{v}$, and $\underline{\tau}$ be scalar-, vector-, and matrix-valued functions, respectively, that are smooth inside each element $K^\pm$. By $(q^\pm, \mathbf{v}^\pm, \underline{\tau}^\pm)$, we denote the traces of $(q, \mathbf{v}, \underline{\tau})$ on F taken from within the interior of $K^\pm$, respectively. Then, we introduce the following averages at $\mathbf{x} \in F$,

$$\{\!\{q\}\!\} = (q^+ + q^-)/2, \qquad \{\!\{\mathbf{v}\}\!\} = (\mathbf{v}^+ + \mathbf{v}^-)/2, \qquad \{\!\{\underline{\tau}\}\!\} = (\underline{\tau}^+ + \underline{\tau}^-)/2.$$

Similarly, the jumps at $\mathbf{x} \in F$ are given by

$$\begin{aligned} [\![q]\!] &= q^+ \mathbf{n}_{K^+} + q^- \mathbf{n}_{K^-}, & [\![\mathbf{v}]\!] &= \mathbf{v}^+ \cdot \mathbf{n}_{K^+} + \mathbf{v}^- \cdot \mathbf{n}_{K^-}, \\ [\![\underline{\mathbf{v}}]\!] &= \mathbf{v}^+ \otimes \mathbf{n}_{K^+} + \mathbf{v}^- \otimes \mathbf{n}_{K^-}, & [\![\underline{\tau}]\!] &= \underline{\tau}^+ \mathbf{n}_{K^+} + \underline{\tau}^- \mathbf{n}_{K^-}. \end{aligned}$$

On boundary faces $F \in \mathcal{F}_\mathcal{D}$, we set $\{\!\{q\}\!\} = q$, $\{\!\{\mathbf{v}\}\!\} = \mathbf{v}$, $\{\!\{\underline{\tau}\}\!\} = \underline{\tau}$, as well as $[\![q]\!] = q\mathbf{n}$, $[\![\mathbf{v}]\!] = \mathbf{v} \cdot \mathbf{n}$, $[\![\underline{\mathbf{v}}]\!] = \mathbf{v} \otimes \mathbf{n}$, and $[\![\underline{\tau}]\!] = \underline{\tau}\mathbf{n}$. Here, $\mathbf{n}$ is the outward unit normal vector on the boundary Γ.

2.4. Discontinuous Galerkin Discretization

Given a mesh $\mathcal{T}_h$ and a polynomial degree $k \geq 1$, we approximate the Stokes problem by finite element functions $(\mathbf{u}_h, p_h) \in \mathbf{V}_h \times Q_h$, where

$$\begin{aligned} \mathbf{V}_h &= \{\, \mathbf{v} \in L^2(\Omega)^d : \mathbf{v}|_K \in \mathcal{Q}^k(K)^d,\ K \in \mathcal{T}_h \,\}, \\ Q_h &= \{\, q \in L^2_0(\Omega) : q|_K \in \mathcal{Q}^{k-1}(K),\ K \in \mathcal{T}_h \,\}. \end{aligned}$$

Here, $\mathcal{Q}^k(K)$ denotes the space of tensor product polynomials on K of degree k in each coordinate direction.

We consider the following discontinuous Galerkin approximation of the Stokes problem: find $(\mathbf{u}_h, p_h) \in \mathbf{V}_h \times Q_h$ such that

$$\left\{ \begin{array}{rcl} A_h(\mathbf{u}_h, \mathbf{v}) \ + \ B_h(\mathbf{v}, p_h) &=& \displaystyle\int_\Omega \mathbf{f} \cdot \mathbf{v}\, d\mathbf{x}, \\ -B_h(\mathbf{u}_h, q) &=& 0 \end{array} \right. \tag{3}$$

for all $(\mathbf{v}, q) \in \mathbf{V}_h \times Q_h$, where

$$\begin{aligned} A_h(\mathbf{u}, \mathbf{v}) &= \nu \int_\Omega \nabla_h \mathbf{u} : \nabla_h \mathbf{v}\, d\mathbf{x} - \int_\mathcal{F} (\{\!\{\nu \nabla_h \mathbf{v}\}\!\} : [\![\underline{\mathbf{u}}]\!] + \{\!\{\nu \nabla_h \mathbf{u}\}\!\} : [\![\underline{\mathbf{v}}]\!]) ds \\ &\quad + \nu \int_\mathcal{F} \gamma \mathtt{h}^{-1} [\![\underline{\mathbf{u}}]\!] : [\![\underline{\mathbf{v}}]\!]\, ds, \\ B_h(\mathbf{v}, q) &= -\int_\Omega q\, \nabla_h \cdot \mathbf{v}\, d\mathbf{x} + \int_\mathcal{F} \{\!\{q\}\!\} [\![\mathbf{v}]\!]\, ds. \end{aligned}$$

Here, ∇_h denotes the discrete nabla operator that is taken elementwise. We further use the notation $\int_{\mathcal{F}} h\,ds = \sum_{F\in\mathcal{F}} \int_F h\,ds$. The function $\gamma \mathtt{h}^{-1}$ is the interior penalty stabilization with $\mathtt{h} \in L^\infty(\mathcal{F})$ denoting the mesh function defined by

$$\mathtt{h}(\mathbf{x}) = \begin{cases} \min\{h_K, h_{K'}\}, & \mathbf{x} \in F \in \mathcal{F}_{\mathcal{I}},\ F = \partial K \cap \partial K', \\ h_K, & \mathbf{x} \in F \in \mathcal{F}_{\mathcal{D}},\ F \subset \partial K, \end{cases}$$

and $\gamma > 0$ a parameter independent of the mesh size. To ensure coercivity of the DG form A_h, the parameter γ must be chosen sufficiently large; see Arnold, Brezzi, Cockburn and Marini [1] and the references cited therein.

It was recently shown that the mixed method defined in (3) satisfies a discrete inf-sup condition, and is thereby well-posed; for details, see Hansbo and Larson [12], Toselli [22], Schötzau, Schwab and Toselli [20] and the references cited therein. Consequently, for (piecewise) smooth analytical Stokes solutions $(\mathbf{u}, p)$, the approximations $(\mathbf{u}_h, p_h)$ obtained from (3) satisfy a priori error bounds that are optimal in the mesh size and almost optimal in the polynomial degree. In polygonal domains in $\mathbb{R}^2$, extensions of these a priori results to Stokes solutions $(\mathbf{u}, p)$ with regularity below $H^2(\Omega)^2 \times H^1(\Omega)$ can be found in Schötzau and Wihler [21]; see also Wihler, Frauenfelder and Schwab [24] for closely related bounds for diffusion problems in non-smooth domains.

REMARK 2.1. *The discontinuous Galerkin form A_h in (3) is also referred to as the interior penalty form. Several other DG forms are available for the discretization of the Laplacian; see Arnold, Brezzi, Cockburn and Marini [1] for a discussion and unifying approach of several DG methods for diffusion problems.*

We further point out that our mixed approximation in (3) is based on so-called mixed-order elements (or $(\mathcal{Q}^k)^d - \mathcal{Q}^{k-1}$ elements), where the approximation degree for the pressure is of one order lower than for the velocity. In view of the approximation properties, this pair is optimally matched. However, by introducing suitable pressure stabilization terms, it is also possible to employ equal-order elements (or $(\mathcal{Q}^k)^d - \mathcal{Q}^k$ elements) with the same approximation degree for the velocity and the pressure; see the LDG approaches by Cockburn, Kanschat, Schötzau and Schwab [7] and Cockburn, Kanschat and Schötzau [6] for details.

REMARK 2.2. *In the case of inhomogeneous Dirichlet boundary conditions, $\mathbf{u} = \mathbf{g}$ on Γ, with a datum $\mathbf{g}$ satisfying the compatibility condition $\int_\Gamma \mathbf{g}\cdot\mathbf{n}\,ds = 0$, the functional on the right-hand side of the first equation in (3) must be replaced by*

$$F_h(\mathbf{v}) = \int_\Omega \mathbf{f}\cdot\mathbf{v}\,d\mathbf{x} - \int_{\mathcal{F}_{\mathcal{D}}} (\mathbf{g}\otimes\mathbf{n}) : (\nu\nabla_h\mathbf{v})\,ds + \nu\int_{\mathcal{F}_{\mathcal{D}}} \gamma\mathtt{h}^{-1}\,\mathbf{g}\cdot\mathbf{v}\,ds.$$

Additionally, the right-hand side of the second equation in (3) is set equal to

$$G_h(q) = -\int_{\mathcal{F}_\mathcal{D}} q\,\mathbf{g}\cdot\mathbf{n}\,ds.$$

3. A Posteriori Error Estimation

In this section we present and discuss an a posteriori estimator for the error measured in terms of the energy norm $|\!|\!| \cdot |\!|\!|_{DG}$ given by

$$|\!|\!|(\mathbf{v},q)|\!|\!|_{DG}^2 = \nu\|\nabla_h\mathbf{v}\|_{0,\Omega}^2 + \nu\gamma\int_{\mathcal{F}} \mathtt{h}^{-1}|\underline{[\![\mathbf{v}]\!]}|^2\,ds + \nu^{-1}\|q\|_{0,\Omega}^2.$$

The following theorem is the main result of this paper.

THEOREM 3.1. *Let $(\mathbf{u},p)\in H_0^1(\Omega)^d\times L_0^2(\Omega)$ be the analytical solution of the Stokes problem (1) and $(\mathbf{u}_h,p_h)\in\mathbf{V}_h\times Q_h$ its mixed DG approximation obtained by (3). Then, the following a posteriori error bound holds:*

$$|\!|\!|(\mathbf{u}-\mathbf{u}_h,p-p_h)|\!|\!|_{DG} \le C_{EST}\Big(\sum_{K\in\mathcal{T}_h}\eta_K^2\Big)^{\frac{1}{2}},$$

where the elemental error indicator η_K is given by

$$\begin{aligned}\eta_K^2 \;=\; & \nu^{-1}h_K^2\|\mathbf{f}+\nu\Delta\mathbf{u}_h-\nabla p_h\|_{0,K}^2+\nu\|\nabla\cdot\mathbf{u}_h\|_{0,K}^2\\ & +\nu^{-1}\|\mathtt{h}^{\frac{1}{2}}([\![p_h]\!]-[\![\nu\nabla_h\mathbf{u}_h]\!])\|_{0,\partial K\setminus\Gamma}^2+\gamma^2\nu\|\mathtt{h}^{-\frac{1}{2}}\underline{[\![\mathbf{u}_h]\!]}\|_{0,\partial K}^2.\end{aligned}$$

Here, the constant $C_{EST}>0$ depends on γ, the inf-sup constant κ in (2), the shape-regularity of the mesh and the polynomial degree k, but is independent of ν and the mesh size.

REMARK 3.1. *For residual-based a posteriori error estimation, the constant C_{EST}, arising in a bound of the type derived in Theorem 3.1, is usually unknown analytically and must be determined numerically for the underlying problem at hand; see Eriksson, Estep, Hansbo and Johnson [9], for example. From the proof of Theorem 3.1, it follows that*

$$C_{EST} = C_S(C_CC_P+C_A)+C_P\gamma^{-1}\max(1,\gamma^{\frac{1}{2}}),$$

where C_S is the stability constant of the problem (cf. Lemma 4.3), C_C is a continuity constant (cf. Lemma 4.2), C_P is a Poincaré constant (cf. Proposition 4.1) and C_A is the constant arising in Proposition 4.2.

REMARK 3.2. *Note that, for simplicity, the error in the approximation of the source term* $\mathbf{f}$ *is not taken into account explicitly in Theorem 3.1. However, this can be done straightforwardly by using the triangle inequality, giving rise to a standard data oscillation term. We point out that, in our numerical results below, the source terms* $\mathbf{f}$ *are always chosen in such a way that the error in the data approximation can be neglected.*

REMARK 3.3. *To incorporate the inhomogeneous boundary condition* $\mathbf{u} = \mathbf{g}$ *on* Γ*, the error indicators* η_K *are simply modified with a corresponding modification of the jump indicators* $\gamma^2\nu\|\mathtt{h}^{-\frac{1}{2}}\underline{[\![\mathbf{u}_h]\!]}\|^2_{0,\partial K}$ *on* $\partial K \cap \Gamma$*, neglecting again data oscillation terms accounting for the approximation of boundary data.*

The proof of Theorem 3.1 is carried out in the next section. It relies on a non-consistent reformulation of the method by using lifting operators in the spirit of Arnold, Brezzi, Cockburn and Marini [1] and then exploiting the recent decomposition result for discontinuous spaces from Houston, Perugia and Schötzau [13]. This is in contrast to the approach of Becker, Hansbo and Larson [3], which is based on employing a suitable Helmholtz decomposition of the error, together with the underlying conservation properties of the DG method, and the approach of Becker, Hansbo and Stenberg [4] that hinges on a saturation assumption on the meshes.

4. Proof of Theorem 3.1

The aim of this section is to prove Theorem 3.1; to this end, we proceed in the following steps.

4.1. Lifting Operators

We begin by suitably extending the forms A_h and B_h to the continuous level using the lifting operators introduced in Arnold, Brezzi, Cockburn and Marini [1]; see also Perugia and Schötzau [18] and Schötzau, Schwab and Toselli [20]. To this end, we define the space

$$\mathbf{V}(h) = H^1_0(\Omega)^d + \mathbf{V}_h, \tag{4}$$

and endow it with the norm

$$\|\mathbf{v}\|^2_{1,h} = \|\nabla_h \mathbf{v}\|^2_{0,\Omega} + \int_{\mathcal{F}} \mathtt{h}^{-1}|\underline{[\![\mathbf{v}]\!]}|^2\,ds.$$

Next, by using the auxiliary space

$$\underline{\Sigma}_h = \{\underline{\tau} \in L^2(\Omega)^{d\times d} : \underline{\tau}|_K \in \mathcal{Q}^k(K)^{d\times d}, K \in \mathcal{T}_h\},$$

we introduce the lifting operator $\underline{\mathcal{L}} : \mathbf{V}(h) \to \underline{\Sigma}_h$ by

$$\int_\Omega \underline{\mathcal{L}}(\mathbf{v}) : \underline{\tau}\, d\mathbf{x} = \int_{\mathcal{F}} \underline{[\![\mathbf{v}]\!]} : \{\!\{\underline{\tau}\}\!\}\, ds \qquad \forall \underline{\tau} \in \underline{\Sigma}_h.$$

In addition, we define $\mathcal{M} : \mathbf{V}(h) \to Q_h$ by

$$\int_\Omega \mathcal{M}(\mathbf{v}) q\, d\mathbf{x} = \int_{\mathcal{F}} [\![\mathbf{v}]\!]\{\!\{q\}\!\}\, ds \qquad \forall q \in Q_h.$$

The above lifting operators have the following stability properties; see Perugia and Schötzau [18] or Schötzau, Schwab and Toselli [20] for details.

LEMMA 4.1. *There exists a constant $C_L > 0$ such that*

$$\|\underline{\mathcal{L}}(\mathbf{v})\|_{0,\Omega}^2 \le C_L \int_{\mathcal{F}} \mathtt{h}^{-1} |\underline{[\![\mathbf{v}]\!]}|^2\, ds, \qquad \|\mathcal{M}(\mathbf{v})\|_{0,\Omega}^2 \le C_L \int_{\mathcal{F}} \mathtt{h}^{-1} |\underline{[\![\mathbf{v}]\!]}|^2\, ds,$$

for any $\mathbf{v} \in \mathbf{V}(h)$. The constant C_L is independent of the mesh size, but depends on the shape-regularity of the mesh and the polynomial degree k.

We are now ready to introduce the following auxiliary forms:

$$\begin{aligned}
\widetilde{A}_h(\mathbf{u},\mathbf{v}) &= \nu \int_\Omega \nabla_h \mathbf{u} : \nabla_h \mathbf{v}\, d\mathbf{x} - \int_\Omega \left(\underline{\mathcal{L}}(\mathbf{u}) : \nu \nabla_h \mathbf{v} + \underline{\mathcal{L}}(\mathbf{v}) : \nu \nabla_h \mathbf{u}\right) d\mathbf{x} \\
&\quad + \nu \int_{\mathcal{F}} \gamma \mathtt{h}^{-1}\, \underline{[\![\mathbf{u}]\!]} : \underline{[\![\mathbf{v}]\!]}\, ds, \\
\widetilde{B}_h(\mathbf{v},q) &= -\int_\Omega q\, \nabla_h \cdot \mathbf{v}\, d\mathbf{x} + \int_\Omega \mathcal{M}(\mathbf{v}) q\, d\mathbf{x}.
\end{aligned}$$

We first point out that, in contrast to A_h and B_h, and A and B, the forms $\widetilde{A}_h$ and $\widetilde{B}_h$ are well-defined on $\mathbf{V}(h) \times \mathbf{V}(h)$ and $\mathbf{V}(h) \times L^2(\Omega)$, respectively. Furthermore, we observe that

$$\widetilde{A}_h = A_h \quad \text{on} \quad \mathbf{V}_h \times \mathbf{V}_h, \qquad \widetilde{A}_h = A \quad \text{on} \quad H_0^1(\Omega)^d \times H_0^1(\Omega)^d,$$

and

$$\widetilde{B}_h = B_h \quad \text{on} \quad \mathbf{V}_h \times Q_h, \qquad \widetilde{B}_h = B \quad \text{on} \quad H_0^1(\Omega)^d \times L_0^2(\Omega).$$

Hence, the form $\widetilde{A}_h$ is an extension of both A_h and A to the space $\mathbf{V}(h) \times \mathbf{V}(h)$, while $\widetilde{B}_h$ extends B_h and B to $\mathbf{V}(h) \times Q(h)$.

Using these auxiliary forms, we may rewrite the discrete problem (3) as follows: find $(\mathbf{u}_h, p_h) \in \mathbf{V}_h \times Q_h$ such that

$$\left\{ \begin{array}{rcl} \widetilde{A}_h(\mathbf{u}_h, \mathbf{v}) \ + \ \widetilde{B}_h(\mathbf{v}, p_h) & = & \displaystyle\int_\Omega \mathbf{f} \cdot \mathbf{v} \, d\mathbf{x}, \\ -\widetilde{B}_h(\mathbf{u}_h, q) & = & 0 \end{array} \right. \tag{5}$$

for all $(\mathbf{v}, q) \in \mathbf{V}_h \times Q_h$.

Then, by setting

$$\mathcal{A}_h(\mathbf{u}, p; \mathbf{v}, q) = \widetilde{A}_h(\mathbf{u}, \mathbf{v}) + \widetilde{B}_h(\mathbf{v}, p) - \widetilde{B}_h(\mathbf{u}, q),$$

for any $(\mathbf{u}, p), (\mathbf{v}, q) \in \mathbf{V}(h) \times L^2(\Omega)$, we may further reformulate problem (3) as follows: find $(\mathbf{u}_h, p_h) \in \mathbf{V}_h \times Q_h$ such that

$$\mathcal{A}_h(\mathbf{u}_h, p_h; \mathbf{v}, q) = \int_\Omega \mathbf{f} \cdot \mathbf{v} \, d\mathbf{x} \tag{6}$$

for all $(\mathbf{v}, q) \in \mathbf{V}_h \times Q_h$. On the discrete spaces $\mathbf{V}_h$ and Q_h, problem (6) is equivalent to (3).

Next, in order to specify how well the analytical solution $(\mathbf{u}, p)$ of the Stokes problem (1) satisfies the formulation in (6), we need to introduce the functional $\mathcal{R}_h$ given by

$$\mathcal{R}_h(\mathbf{u}, p; \mathbf{v}, q) = \mathcal{A}_h(\mathbf{u}, p; \mathbf{v}, q) - \int_\Omega \mathbf{f} \cdot \mathbf{v} \, d\mathbf{x}, \qquad (\mathbf{v}, q) \in \mathbf{V}_h \times Q_h. \tag{7}$$

We will then make use of the following error equation:

$$\mathcal{A}_h(\mathbf{u} - \mathbf{u}_h, p - p_h; \mathbf{v}, q) = \mathcal{R}_h(\mathbf{u}, p; \mathbf{v}, q), \qquad (\mathbf{v}, q) \in \mathbf{V}_h \times Q_h. \tag{8}$$

Using the results of Section 8 of Schötzau, Schwab and Toselli [20], it can be seen that, for a sufficiently smooth analytical solution $(\mathbf{u}, p)$ to the Stokes problem, there holds

$$\mathcal{R}_h(\mathbf{u}, p; \mathbf{v}, q) = \nu \int_{\mathcal{F}} \{\!\{ \nabla_h \mathbf{u} - \underline{\Pi}(\nabla_h \mathbf{u}) \}\!\} : \underline{[\![\mathbf{v}]\!]} \, ds - \int_{\mathcal{F}} \{\!\{ p - \Pi p \}\!\} [\![\mathbf{v}]\!] \, ds$$

for all $\mathbf{v} \times q \in \mathbf{V}_h \times Q_h$, where $\underline{\Pi}$ and Π denote the L^2-projection operators onto $\underline{\Sigma}_h$ and Q_h, respectively. Hence, the functional $\mathcal{R}_h$ is in fact independent of $q \in Q_h$ and $\mathcal{R}_h(\mathbf{u}, p; \mathbf{v}, q) = 0$ for any $\mathbf{v} \in \mathbf{V}_h \cap H_0^1(\Omega)^d$.

4.2. Stability Results

In this section, we collect some basic stability properties of the form $\mathcal{A}_h$. First of all, we have the following continuity result:

LEMMA 4.2. *For any* $(\mathbf{u},p),(\mathbf{v},q)\in\mathbf{V}(h)\times L^2(\Omega)$*, there holds*

$$|\mathcal{A}_h(\mathbf{u},p;\mathbf{v},q)|\leq C_C|\!|\!|(\mathbf{u},p)|\!|\!|_{DG}|\!|\!|(\mathbf{v},q)|\!|\!|_{DG},$$

with $C_C=\max(2+d,1+2C_L\gamma^{-1})$*, where* C_L *is the constant arising in Lemma 4.1.*

Proof. From the stability estimates for $\underline{\mathcal{L}}$ and $\mathcal{M}$ in Lemma 4.1, the definition of the forms $\widetilde{A}_h$ and $\widetilde{B}_h$, and the Cauchy-Schwarz inequality, we readily obtain

$$\begin{aligned}|\mathcal{A}_h(\mathbf{u},p;\mathbf{v},q)| \;\leq\; &\left(2\nu\|\nabla_h\mathbf{u}\|_{0,\Omega}^2+\nu(2C_L\gamma^{-1}+1)\int_{\mathcal{F}_h}\gamma\mathtt{h}^{-1}|\underline{[\![\mathbf{u}]\!]}|^2\,ds\right.\\ &\left.+\nu\|\nabla_h\cdot\mathbf{u}\|_{0,\Omega}^2+2\nu^{-1}\|p\|_{0,\Omega}^2\right)^{\frac12}\\ &\times\left(2\nu\|\nabla_h\mathbf{v}\|_{0,\Omega}^2+\nu(2C_L\gamma^{-1}+1)\int_{\mathcal{F}_h}\gamma\mathtt{h}^{-1}|\underline{[\![\mathbf{v}]\!]}|^2\,ds\right.\\ &\left.+\nu\|\nabla_h\cdot\mathbf{v}\|_{0,\Omega}^2+2\nu^{-1}\|q\|_{0,\Omega}^2\right)^{\frac12}.\end{aligned}$$

Since $\|\nabla_h\cdot\mathbf{u}\|_{0,\Omega}^2\leq d\|\nabla_h\mathbf{u}\|_{0,\Omega}^2$ and $\|\nabla_h\cdot\mathbf{v}\|_{0,\Omega}^2\leq d\|\nabla_h\mathbf{v}\|_{0,\Omega}^2$, the claim follows. □

Next, we recall the following stability result for the form $\mathcal{A}_h$ restricted to $H_0^1(\Omega)^d\times L_0^2(\Omega)$. This result is a direct consequence of the definition of the auxiliary forms $\widetilde{A}_h$ and $\widetilde{B}_h$ and the inf-sup condition in (2).

LEMMA 4.3. *There exists a stability constant* $C_S>0$ *such that for any* $(\mathbf{u},p)\in H_0^1(\Omega)^d\times L_0^2(\Omega)$*, there is* $(\mathbf{v},q)\in H_0^1(\Omega)^d\times L_0^2(\Omega)$ *with*

$$\mathcal{A}_h(\mathbf{u},p;\mathbf{v},q)\geq|\!|\!|(\mathbf{u},p)|\!|\!|_{DG},\qquad|\!|\!|(\mathbf{v},q)|\!|\!|_{DG}\leq C_S.$$

The constant C_S *is independent of* ν*,* γ *and the mesh size, but depends on the inf-sup constant* κ *in (2).*

Proof. Let $p\in L_0^2(\Omega)$. Then, referring to (2) there exists $\mathbf{w}\in H_0^1(\Omega)^d$ such that

$$-\int_\Omega p\nabla\cdot\mathbf{w}\,d\mathbf{x}\geq\kappa\|p\|_{0,\Omega}^2,\qquad\|\mathbf{w}\|_{1,h}=\|\nabla\mathbf{w}\|_{0,\Omega}\leq\|p\|_{0,\Omega}.\tag{9}$$

Now, we choose

$$\widehat{\mathbf{v}}=\alpha\mathbf{u}+\nu^{-1}\beta\mathbf{w},\qquad\widehat{q}=\alpha p,$$

with

$$\alpha = 1 + \kappa^{-2}, \qquad \beta = 2\kappa^{-1}.$$

Since $\mathbf{u}$ and $\widehat{\mathbf{v}}$ are in $H_0^1(\Omega)^d$, we have that $\underline{\mathcal{L}}(\mathbf{u}) = \underline{\mathcal{L}}(\widehat{\mathbf{v}}) = \underline{0}$ and $\mathcal{M}(\mathbf{u}) = \mathcal{M}(\widehat{\mathbf{v}}) = 0$, together with $\underline{[\![\mathbf{u}]\!]} = \underline{[\![\widehat{\mathbf{v}}]\!]} = \underline{0}$ on $\mathcal{F}$. Hence, using the bounds in (9) and the arithmetic-geometric mean inequality, we obtain

$$\begin{aligned}
\mathcal{A}_h(\mathbf{u},p;\widehat{\mathbf{v}},\widehat{q}) &= \nu\int_\Omega \nabla\mathbf{u} : \nabla\widehat{\mathbf{v}}\,d\mathbf{x} - \int_\Omega p\nabla\cdot\widehat{\mathbf{v}}\,d\mathbf{x} + \int_\Omega \widehat{q}\nabla\cdot\mathbf{u}\,d\mathbf{x}\\
&= \nu\alpha\|\mathbf{u}\|_{1,h}^2 + \beta\int_\Omega \nabla\mathbf{u} : \nabla\mathbf{w}\,d\mathbf{x} - \nu^{-1}\beta\int_\Omega p\nabla\cdot\mathbf{w}\,d\mathbf{x}\\
&\geq \Big(\nu\alpha - \frac{\nu\beta}{2\kappa}\Big)\|\mathbf{u}\|_{1,h}^2 - \frac{\beta\nu^{-1}\kappa}{2}\|\mathbf{w}\|_{1,h}^2 + \beta\nu^{-1}\kappa\|p\|_{0,\Omega}^2\\
&\geq \Big(\alpha - \frac{\beta}{2\kappa}\Big)\nu\|\mathbf{u}\|_{1,h}^2 + \frac{1}{2}\beta\nu^{-1}\kappa\|p\|_{0,\Omega}^2\\
&= |\!|\!|(\mathbf{u},p)|\!|\!|_{DG}^2.
\end{aligned}$$

Furthermore, employing the triangle inequality, we get

$$\begin{aligned}
|\!|\!|(\widehat{\mathbf{v}},\widehat{q})|\!|\!|_{DG}^2 &= \nu\|\widehat{\mathbf{v}}\|_{1,h}^2 + \nu^{-1}\|\widehat{q}\|_{0,\Omega}^2\\
&\leq 2\nu\alpha^2\|\mathbf{u}\|_{1,h}^2 + 2\nu^{-1}\beta^2\|\mathbf{w}\|_{1,h}^2 + \nu^{-1}\alpha^2\|p\|_{0,\Omega}^2\\
&\leq 2\nu\alpha^2\|\mathbf{u}\|_{1,h}^2 + (2\beta^2+\alpha^2)\nu^{-1}\|p\|_{0,\Omega}^2\\
&\leq \max(2\alpha^2, 2\beta^2+\alpha^2)|\!|\!|(\mathbf{u},p)|\!|\!|_{DG}^2.
\end{aligned}$$

Setting $(\mathbf{v},q) = |\!|\!|(\mathbf{u},p)|\!|\!|_{DG}^{-1}(\widehat{\mathbf{v}},\widehat{q})$, completes the proof with the stability constant C_S given by $C_S^2 = \max(2\alpha^2, 2\beta^2+\alpha^2)$. □

Finally, we state a decomposition result for discontinuous finite element spaces. To this end, let $\mathbf{V}_h^c = \mathbf{V}_h \cap H_0^1(\Omega)^d$. The orthogonal complement in $\mathbf{V}_h$ of $\mathbf{V}_h^c$ with respect to the norm $\|\cdot\|_{1,h}$ is denoted by $\mathbf{V}_h^\perp$. For meshes with 1-irregular hanging nodes, as assumed in this paper, the following equivalence result holds. The proof can be found in Houston, Perugia and Schötzau [13]; it crucially relies on an approximation result of Karakashian and Pascal [17, Section 2.1].

PROPOSITION 4.1. *The expression*

$$\mathbf{v} \mapsto \Big(\int_{\mathcal{F}} \mathtt{h}^{-1}|\underline{[\![\mathbf{v}]\!]}|^2\,ds\Big)^{\frac{1}{2}}$$

is a norm on $\mathbf{V}_h^\perp$. This norm is equivalent to the norm $\|\cdot\|_{1,h}$ and there is a constant $C_P > 0$ such that

$$\|\mathbf{v}\|_{1,h} \leq C_P\Big(\int_{\mathcal{F}} \mathtt{h}^{-1}|\underline{[\![\mathbf{v}]\!]}|^2\,ds\Big)^{\frac{1}{2}} \leq C_P\|\mathbf{v}\|_{1,h},$$

for all $\mathbf{v} \in \mathbf{V}_h^{\perp}$. *The constant* C_P *is independent of the mesh size, but depends on the shape-regularity of the mesh and the polynomial degree* k.

REMARK 4.1. *While the result in Proposition 4.1 holds for meshes with* 1*-irregular hanging nodes (see Karakashian and Pascal [17, Section 2.1]), it is unknown whether it holds on completely non-matching meshes as the ones considered by Becker, Hansbo and Stenberg [4] for diffusion problems. On the other hand, the approach there is based on a saturation assumption on the meshes that is not present in our analysis.*

4.3. An Auxiliary Result

Next, we prove an auxiliary result. To this end, we let $(\mathbf{v}, q) \in H_0^1(\Omega)^d \times L_0^2(\Omega)$ be arbitrary; further, we write $(\mathbf{v}_h, q_h) \in \mathbf{V}_h \times Q_h$ to denote an approximation to $(\mathbf{v}, q)$ satisfying

$$\sum_{K\in\mathcal{T}_h} (h_K^{-2}\|\mathbf{v}-\mathbf{v}_h\|_{0,K}^2 + \|\nabla(\mathbf{v}-\mathbf{v}_h)\|_{0,K}^2 + \|\mathtt{h}^{-\frac{1}{2}}(\mathbf{v}-\mathbf{v}_h)\|_{0,\partial K}^2) \quad (10)$$
$$\leq C_I^2\|\nabla\mathbf{v}\|_{0,\Omega}^2,$$

as well as,

$$\|q - q_h\|_{0,\Omega} \leq C_I\|q\|_{0,\Omega}, \quad (11)$$

with an interpolation constant C_I, which is independent of the mesh size, but depends on the shape-regularity of the mesh and the polynomial degree k. These assumptions are satisfied, for example, if $\mathbf{v}_h$ and q_h are chosen to be L^2-projections of $\mathbf{v}$ and q onto $\mathbf{V}_h$ and Q_h, respectively.

PROPOSITION 4.2. *Under the foregoing assumptions (10) and (11), the following inequality holds*

$$\left|\int_\Omega \mathbf{f}\cdot(\mathbf{v}-\mathbf{v}_h)\,d\mathbf{x} - \mathcal{A}_h(\mathbf{u}_h, p_h; \mathbf{v}-\mathbf{v}_h, q-q_h)\right|$$
$$\leq C_A\Big(\sum_{K\in\mathcal{T}_h}\eta_K^2\Big)^{\frac{1}{2}}|\!|\!|(\mathbf{v},q)|\!|\!|_{DG}.$$

Here, $C_A = C_I\left(\frac{5}{2}(1+2C_L\gamma^{-2})\right)^{\frac{1}{2}}$, *where* C_I *and* C_L *are the constants from (10), (11) and from Lemma 4.1, respectively.*

Proof. We set $\xi_{\mathbf{v}} = \mathbf{v} - \mathbf{v}_h$, $\xi_q = q - q_h$, and

$$T = \int_\Omega \mathbf{f}\cdot\xi_{\mathbf{v}}\,d\mathbf{x} - \mathcal{A}_h(\mathbf{u}_h, p_h; \xi_{\mathbf{v}}, \xi_q).$$

We first note that

$$T = \int_\Omega \mathbf{f}\cdot\xi_{\mathbf{v}}\,d\mathbf{x} - \widetilde{A}_h(\mathbf{u}_h,\xi_{\mathbf{v}}) - \widetilde{B}_h(\xi_{\mathbf{v}},p_h) + \widetilde{B}_h(\mathbf{u}_h,\xi_q). \tag{12}$$

Integration by parts and the definition of the lifting operator $\underline{\mathcal{L}}$ leads to

$$\begin{aligned}
-\widetilde{A}_h(\mathbf{u}_h,\xi_{\mathbf{v}}) &= \sum_{K\in\mathcal{T}_h}\left(\int_K \nu\Delta\mathbf{u}_h\cdot\xi_{\mathbf{v}}\,d\mathbf{x} - \int_{\partial K}\nu\nabla_h\mathbf{u}_h : (\xi_{\mathbf{v}}\otimes\mathbf{n}_K)ds\right)\\
&\quad + \int_\Omega \nu\mathcal{L}(\mathbf{u}_h):\nabla_h\xi_{\mathbf{v}}\,d\mathbf{x} + \int_\Omega \nu\mathcal{L}(\xi_{\mathbf{v}}):\nabla_h\mathbf{u}_h\,d\mathbf{x}\\
&\quad - \nu\int_{\mathcal{F}}\gamma\mathtt{h}^{-1}\,\underline{[\![\mathbf{u}_h]\!]}:\underline{[\![\xi_{\mathbf{v}}]\!]}\,ds\\
&= \sum_{K\in\mathcal{T}_h}\int_K \nu\Delta\mathbf{u}_h\cdot\xi_{\mathbf{v}}\,d\mathbf{x} - \int_{\mathcal{F}_\mathcal{I}}[\![\nu\nabla_h\mathbf{u}_h]\!]\cdot\{\!\{\xi_{\mathbf{v}}\}\!\}\,ds\\
&\quad + \int_\Omega \nu\mathcal{L}(\mathbf{u}_h):\nabla_h\xi_{\mathbf{v}}\,d\mathbf{x} - \nu\int_{\mathcal{F}}\gamma\mathtt{h}^{-1}\,\underline{[\![\mathbf{u}_h]\!]}:\underline{[\![\xi_{\mathbf{v}}]\!]}\,ds.
\end{aligned}$$

Similarly, by integration by parts, we obtain

$$\begin{aligned}
-\widetilde{B}_h(\xi_{\mathbf{v}},p_h) + \widetilde{B}_h(\mathbf{u}_h,\xi_q) &= -\sum_{K\in\mathcal{T}_h}\int_K \nabla p_h\cdot\xi_{\mathbf{v}}\,d\mathbf{x} + \int_{\mathcal{F}_\mathcal{I}}[\![p_h]\!]\cdot\{\!\{\xi_{\mathbf{v}}\}\!\}\,ds\\
&\quad - \sum_{K\in\mathcal{T}_h}\int_K \xi_q\nabla\cdot\mathbf{u}_h\,d\mathbf{x} + \int_\Omega \mathcal{M}(\mathbf{u}_h)\xi_q\,d\mathbf{x}.
\end{aligned}$$

Substituting the above expressions into (12), we get

$$\begin{aligned}
T &= \sum_{K\in\mathcal{T}_h}\int_K (\mathbf{f}+\nu\Delta\mathbf{u}_h-\nabla p_h)\cdot\xi_{\mathbf{v}}\,d\mathbf{x} - \sum_{K\in\mathcal{T}_h}\int_K \xi_q\nabla\cdot\mathbf{u}_h\,d\mathbf{x}\\
&\quad + \int_{\mathcal{F}_\mathcal{I}}([\![p_h]\!] - [\![\nu\nabla_h\mathbf{u}_h]\!])\cdot\{\!\{\xi_{\mathbf{v}}\}\!\}\,ds - \nu\int_{\mathcal{F}}\gamma\mathtt{h}^{-1}\underline{[\![\mathbf{u}_h]\!]}:\underline{[\![\xi_{\mathbf{v}}]\!]}\,ds\\
&\quad + \int_\Omega \nu\mathcal{L}(\mathbf{u}_h):\nabla_h\xi_{\mathbf{v}}\,d\mathbf{x} + \int_\Omega \mathcal{M}(\mathbf{u}_h)\xi_q\,d\mathbf{x}.
\end{aligned}$$

Using the stability bounds from Lemma 4.1, we obtain

$$\begin{aligned}
|T| &\le \sum_{K\in\mathcal{T}_h}\nu^{-\frac12}h_K\|\mathbf{f}+\nu\Delta\mathbf{u}_h-\nabla p_h\|_{0,K}\,\nu^{\frac12}h_K^{-1}\|\xi_{\mathbf{v}}\|_{0,K}\\
&\quad + \sum_{K\in\mathcal{T}_h}\nu^{\frac12}\|\nabla\cdot\mathbf{u}_h\|_{0,K}\,\nu^{-\frac12}\|\xi_q\|_{0,K}\\
&\quad + \sum_{F\in\mathcal{F}_\mathcal{I}}\nu^{-\frac12}\|\mathtt{h}^{\frac12}([\![p_h]\!]-[\![\nu\nabla_h\mathbf{u}_h]\!])\|_{0,F}\,\nu^{\frac12}\|\mathtt{h}^{-\frac12}\{\!\{\xi_{\mathbf{v}}\}\!\}\|_{0,F}
\end{aligned}$$

$$+\sum_{F\in\mathcal{F}}\gamma\nu^{\frac{1}{2}}\|\mathtt{h}^{-\frac{1}{2}}\underline{[\![\mathbf{u}_h]\!]}\|_{0,F}\,\nu^{\frac{1}{2}}\|\mathtt{h}^{-\frac{1}{2}}\underline{[\![\xi_{\mathbf{v}}]\!]}\|_{0,F}$$

$$+\nu^{\frac{1}{2}}C_L^{\frac{1}{2}}\left(\sum_{F\in\mathcal{F}}\|\mathtt{h}^{-\frac{1}{2}}\underline{[\![\mathbf{u}_h]\!]}\|_{0,F}^2\right)^{\frac{1}{2}}\nu^{\frac{1}{2}}\|\nabla_h\xi_{\mathbf{v}}\|_{0,\Omega}$$

$$+\nu^{\frac{1}{2}}C_L^{\frac{1}{2}}\left(\sum_{F\in\mathcal{F}}\|\mathtt{h}^{-\frac{1}{2}}\underline{[\![\mathbf{u}_h]\!]}\|_{0,F}^2\right)^{\frac{1}{2}}\nu^{-\frac{1}{2}}\|\xi_q\|_{0,\Omega}.$$

Applying the Cauchy-Schwarz inequality, results in

$$\begin{aligned}|T| \;\le\; &\left(\sum_{K\in\mathcal{T}_h}\left(\nu^{-1}h_K^2\|\mathbf{f}+\nu\Delta\mathbf{u}_h-\nabla p_h\|_{0,K}^2+\nu\|\nabla\cdot\mathbf{u}_h\|_{0,K}^2\right)\right.\\
&+\nu^{-1}\sum_{F\in\mathcal{F}_{\mathcal{I}}}\|\mathtt{h}^{\frac{1}{2}}([\![p_h]\!]-[\![\nu\nabla_h\mathbf{u}_h]\!])\|_{0,F}^2\\
&\left.+(1+2C_L\gamma^{-2})\nu\gamma^2\sum_{F\in\mathcal{F}}\|\mathtt{h}^{-\frac{1}{2}}\underline{[\![\mathbf{u}_h]\!]}\|_{0,F}^2\right)^{\frac{1}{2}}\\
&\times\left(\sum_{K\in\mathcal{T}_h}\left(\nu h_K^{-2}\|\xi_{\mathbf{v}}\|_{0,K}^2+\nu\|\nabla\xi_{\mathbf{v}}\|_{0,K}^2+2\nu^{-1}\|\xi_q\|_{0,K}^2\right)\right.\\
&\left.+\nu\sum_{F\in\mathcal{F}_{\mathcal{I}}}\|\mathtt{h}^{-\frac{1}{2}}\{\!\{\xi_{\mathbf{v}}\}\!\}\|_{0,F}^2+\nu\sum_{F\in\mathcal{F}}\|\mathtt{h}^{-\frac{1}{2}}\underline{[\![\xi_{\mathbf{v}}]\!]}\|_{0,F}^2\right)^{\frac{1}{2}}.\end{aligned}$$

In addition, noticing that

$$\begin{aligned}\sum_{F\in\mathcal{F}_{\mathcal{I}}}\|\mathtt{h}^{\frac{1}{2}}([\![p_h]\!]-[\![\nu\nabla_h\mathbf{u}_h]\!])\|_{0,F}^2 \;&=\; \frac{1}{2}\sum_{K\in\mathcal{T}_h}\|\mathtt{h}^{\frac{1}{2}}([\![p_h]\!]-[\![\nu\nabla_h\mathbf{u}_h]\!])\|_{0,\partial K\setminus\Gamma}^2,\\
\sum_{F\in\mathcal{F}}\|\mathtt{h}^{-\frac{1}{2}}\underline{[\![\mathbf{u}_h]\!]}\|_{0,F}^2 \;&\le\; \sum_{K\in\mathcal{T}_h}\|\mathtt{h}^{-\frac{1}{2}}\underline{[\![\mathbf{u}_h]\!]}\|_{0,\partial K}^2,\end{aligned}\tag{13}$$

and

$$\begin{aligned}\sum_{F\in\mathcal{F}_{\mathcal{I}}}\|\mathtt{h}^{-\frac{1}{2}}\{\!\{\xi_{\mathbf{v}}\}\!\}\|_{0,F}^2 \;&\le\; \frac{1}{2}\sum_{K\in\mathcal{T}_h}\|\mathtt{h}^{-\frac{1}{2}}\xi_{\mathbf{v}}\|_{0,\partial K}^2,\\
\sum_{F\in\mathcal{F}}\|\mathtt{h}^{-\frac{1}{2}}\underline{[\![\xi_{\mathbf{v}}]\!]}\|_{0,F}^2 \;&\le\; 2\sum_{K\in\mathcal{T}_h}\|\mathtt{h}^{-\frac{1}{2}}\xi_{\mathbf{v}}\|_{0,\partial K}^2,\end{aligned}$$

leads to

$$|T| \;\le\; \left(\sum_{K\in\mathcal{T}_h}\nu^{-1}h_K^2\|\mathbf{f}+\nu\Delta\mathbf{u}_h-\nabla p_h\|_{0,K}+\nu\|\nabla_h\cdot\mathbf{u}\|_{0,K}^2\right.$$

$$
\begin{aligned}
&+\frac{1}{2}\nu^{-1}\|\mathtt{h}^{\frac{1}{2}}(\llbracket p_h\rrbracket - \llbracket \nu\nabla_h \mathbf{u}_h\rrbracket)\|^2_{0,\partial K\setminus\Gamma}\\
&+(1+2C_L\gamma^{-2})\nu\gamma^2\|\mathtt{h}^{-\frac{1}{2}}\underline{\llbracket \mathbf{u}_h\rrbracket}\|^2_{0,\partial K}\Bigg)^{\frac{1}{2}}\\
&\times\Bigg(\sum_{K\in\mathcal{T}_h}\nu\left(h_K^{-2}\|\xi_{\mathbf{v}}\|^2_{0,K}+\|\nabla\xi_{\mathbf{v}}\|^2_{0,K}+\frac{5}{2}\|\mathtt{h}^{-\frac{1}{2}}\xi_{\mathbf{v}}\|^2_{0,\partial K}\right)\\
&\qquad+2\nu^{-1}\|\xi_q\|^2_{0,K}\Bigg)^{\frac{1}{2}}\\
\leq\ &\left(\frac{5}{2}\left(1+2C_L\gamma^{-2}\right)\right)^{\frac{1}{2}}\left(\sum_{K\in\mathcal{T}_h}\eta_K^2\right)^{\frac{1}{2}}\\
&\times\Bigg(\sum_{K\in\mathcal{T}_h}\nu\left(h_K^{-2}\|\xi_{\mathbf{v}}\|^2_{0,K}+\|\nabla\xi_{\mathbf{v}}\|^2_{0,K}+\|\mathtt{h}^{-\frac{1}{2}}\xi_{\mathbf{v}}\|^2_{0,\partial K}\right)\\
&\qquad+\nu^{-1}\|\xi_q\|^2_{0,K}\Bigg)^{\frac{1}{2}}.
\end{aligned}
$$

Making use of the approximation properties in (10) and (11) completes the proof. □

4.4. A Posteriori Error Estimation

In this section we complete the proof of Theorem 3.1. To this end, we denote the error of the DG approximation by $(\mathbf{e}_u, e_p) = (\mathbf{u}-\mathbf{u}_h, p-p_h)$. Furthermore, we decompose $\mathbf{u}_h$ into $\mathbf{u}_h = \mathbf{u}_h^c \oplus \mathbf{u}_h^\perp$, in accordance with the decomposition in Section 4.2 and Proposition 4.1. We then set $\mathbf{e}_u^c = \mathbf{u} - \mathbf{u}_h^c$.

Using the equivalence result in Proposition 4.1, the fact that $\underline{\llbracket \mathbf{u}_h\rrbracket} = \underline{\llbracket \mathbf{u}_h^\perp\rrbracket}$ and the inequality (13), we have

$$
\begin{aligned}
|\!|\!|(\mathbf{e}_u, e_p)|\!|\!|_{DG} &\leq |\!|\!|(\mathbf{e}_u^c, e_p)|\!|\!|_{DG} + \nu^{\frac{1}{2}}\max(1,\gamma^{\frac{1}{2}})\|\mathbf{u}_h^\perp\|_{1,h}\\
&\leq |\!|\!|(\mathbf{e}_u^c, e_p)|\!|\!|_{DG} + C_P\max(1,\gamma^{\frac{1}{2}})\left(\nu\int_{\mathcal{F}}\mathtt{h}^{-1}|\underline{\llbracket \mathbf{u}_h\rrbracket}|^2\,ds\right)^{\frac{1}{2}}\\
&\leq |\!|\!|(\mathbf{e}_u^c, e_p)|\!|\!|_{DG} + C_P\gamma^{-1}\max(1,\gamma^{\frac{1}{2}})\left(\sum_{K\in\mathcal{T}_h}\eta_K^2\right)^{\frac{1}{2}}.
\end{aligned}
$$

To bound the term $|\!|\!|(\mathbf{e}_u^c, e_p)|\!|\!|_{DG}$, we invoke the stability result from Lemma 4.3 which gives us a function $(\mathbf{v}, q) \in H_0^1(\Omega)^d \times L_0^2(\Omega)$ such

that

$$|\!|\!|(\mathbf{e}_u^c, e_p)|\!|\!|_{DG} \leq \mathcal{A}_h(\mathbf{e}_u^c, e_p; \mathbf{v}, q), \qquad |\!|\!|(\mathbf{v}, q)|\!|\!|_{DG} \leq C_S. \tag{14}$$

Let $(\mathbf{v}_h, q_h) \in \mathbf{V}_h \times Q_h$ be arbitrary. Elementary manipulations, combined with the error equation (8), lead to

$$\begin{aligned}
|\!|\!|(\mathbf{e}_u^c, e_p)|\!|\!|_{DG} &\leq \mathcal{A}_h(\mathbf{e}_u^c, e_p; \mathbf{v}, q) \\
&= \mathcal{A}_h(\mathbf{e}_u, e_p; \mathbf{v}, q) + \mathcal{A}_h(\mathbf{u}_h^\perp, 0; \mathbf{v}, q) \\
&= \mathcal{A}_h(\mathbf{e}_u, e_p; \mathbf{v} - \mathbf{v}_h, q - q_h) + \mathcal{R}_h(\mathbf{u}, p; \mathbf{v}_h, q_h) \\
&\quad + \mathcal{A}_h(\mathbf{u}_h^\perp, 0; \mathbf{v}, q) \\
&= \mathcal{A}_h(\mathbf{u}, p; \mathbf{v} - \mathbf{v}_h, q - q_h) - \mathcal{A}_h(\mathbf{u}_h, p_h; \mathbf{v} - \mathbf{v}_h, q - q_h) \\
&\quad + \mathcal{R}_h(\mathbf{u}, p; \mathbf{v}_h, q_h) + \mathcal{A}_h(\mathbf{u}_h^\perp, 0; \mathbf{v}, q).
\end{aligned}$$

Since $(\mathbf{v}, q) \in H_0^1(\Omega)^d \times L_0^2(\Omega)$, we note that, with the definition (7) of $\mathcal{R}_h$ and the weak formulation of the Stokes problem,

$$\begin{aligned}
\mathcal{A}_h(\mathbf{u}, p; \mathbf{v} - \mathbf{v}_h, q - q_h) &= \mathcal{A}_h(\mathbf{u}, p; \mathbf{v}, q) - \mathcal{A}_h(\mathbf{u}, p; \mathbf{v}_h, q_h) \\
&= \int_\Omega \mathbf{f} \cdot (\mathbf{v} - \mathbf{v}_h)\, d\mathbf{x} - \mathcal{R}_h(\mathbf{u}, p; \mathbf{v}_h, q_h).
\end{aligned}$$

Therefore,

$$\begin{aligned}
|\!|\!|(\mathbf{e}_u^c, e_p)|\!|\!|_{DG} &\leq \int_\Omega \mathbf{f} \cdot (\mathbf{v} - \mathbf{v}_h)\, d\mathbf{x} - \mathcal{A}_h(\mathbf{u}_h, p_h; \mathbf{v} - \mathbf{v}_h, q - q_h) \\
&\quad + \mathcal{A}_h(\mathbf{u}_h^\perp, 0; \mathbf{v}, q).
\end{aligned}$$

Choosing $\mathbf{v}_h$ and q_h as in (10) and (11) yields

$$\begin{aligned}
|\!|\!|(\mathbf{e}_u^c, e_p)|\!|\!|_{DG} &\leq |\mathcal{A}_h(\mathbf{u}_h^\perp, 0; \mathbf{v}, q)| \\
&\quad + \left| \int_\Omega \mathbf{f} \cdot (\mathbf{v} - \mathbf{v}_h)\, d\mathbf{x} - \mathcal{A}_h(\mathbf{u}_h, p_h; \mathbf{v} - \mathbf{v}_h, q - q_h) \right| \\
&\leq C_C \nu^{\frac{1}{2}} \|\mathbf{u}_h^\perp\|_{1,h} |\!|\!|(\mathbf{v}, q)|\!|\!|_{DG} \\
&\quad + C_A \left(\sum_{K \in \mathcal{T}_h} \eta_K^2 \right)^{\frac{1}{2}} |\!|\!|(\mathbf{v}, q)|\!|\!|_{DG} \\
&\leq (C_C C_P + C_A) \left(\sum_{K \in \mathcal{T}_h} \eta_K^2 \right)^{\frac{1}{2}} |\!|\!|(\mathbf{v}, q)|\!|\!|_{DG}.
\end{aligned}$$

Here, we have used the continuity of $\mathcal{A}_h$ from Lemma 4.2, the equivalence result from Proposition 4.1 and the auxiliary result from Proposition 4.2. Using the bound (14) for $(\mathbf{v}, q)$ gives

$$|\!|\!|(\mathbf{e}_u^c, e_p)|\!|\!|_{DG} \leq C_S (C_C C_P + C_A) \left(\sum_{K \in \mathcal{T}_h} \eta_K^2 \right)^{\frac{1}{2}},$$

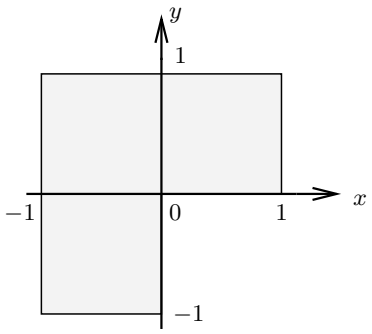

Figure 1. L–shaped domain Ω.

which completes the proof of Theorem 3.1.

5. Numerical Experiments

In this section we present a series of two-dimensional numerical examples to illustrate the practical performance of the proposed a posteriori error estimator within an automatic adaptive refinement procedure. In each of the examples shown below, we set the polynomial degree k equal to 1. The DG solution of (3) is computed using the value $\gamma = 10$. The adaptive meshes are constructed by employing the fixed fraction strategy, with refinement and unrefinement fractions set to 25% and 10%, respectively. Here, the emphasis will be to demonstrate that the proposed a posteriori error indicator converges to zero at the same asymptotic rate as the energy norm of the actual error on a sequence of non-uniform adaptively refined meshes. For simplicity, we always choose $\gamma = 1$ to evaluate the local estimators and the energy norm. Furthermore, as in Becker, Hansbo and Larson [3], we set the constant C_{EST} arising in Theorem 3.1 equal to one and ensure that the corresponding effectivity indices are roughly constant on all of the meshes employed; here, the effectivity index is defined as the ratio of the a posteriori error bound and the energy norm of the actual error. In general, to ensure the reliability of the error estimator, C_{EST} must be determined numerically for the underlying problem at hand, cf. Eriksson, Estep, Hansbo and Johnson [9], for example.

5.1. Example 1

Here, we let $\Omega \subset \mathbb{R}^2$ be the L–shaped domain shown in Figure 1; further, we select $\nu = 1$, $\mathbf{f} = \mathbf{0}$ and enforce appropriate inhomogeneous boundary conditions for $\mathbf{u}$ on Γ so that the analytical solution to (1)

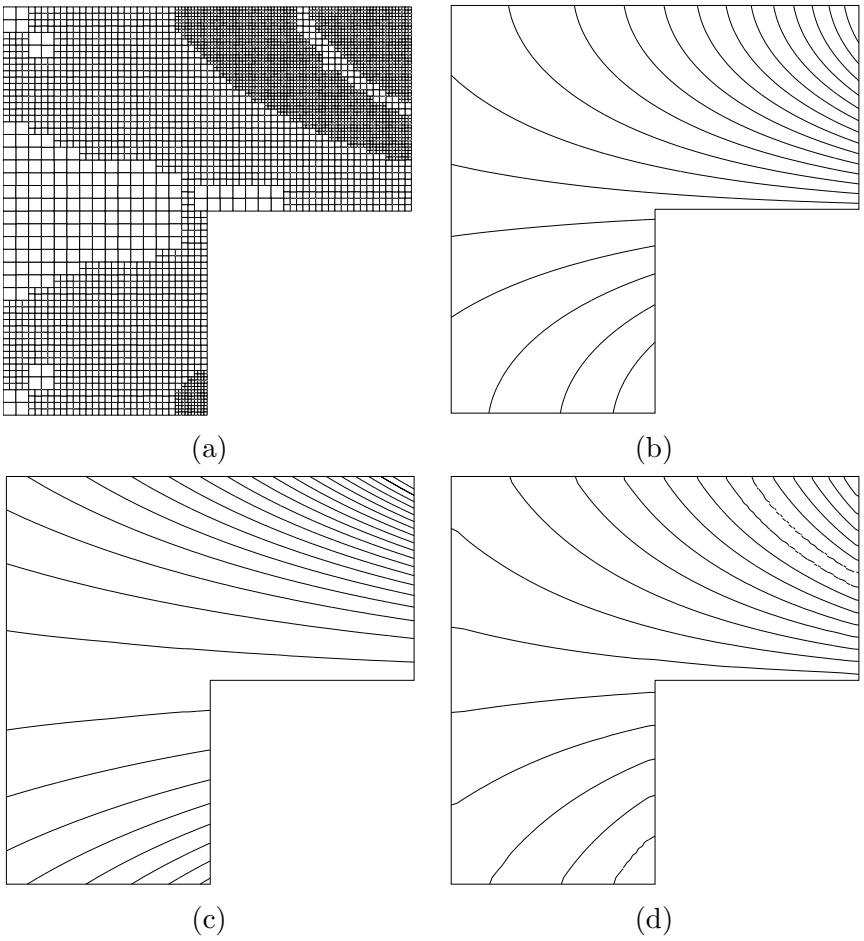

Figure 2. Example 1. (a) Computational mesh with 4359 elements, after 10 adaptive refinements. Numerical approximation to: (b) $\mathbf{u}_1$; (c) $\mathbf{u}_2$; (d) p.

is given by

$$\begin{pmatrix} \mathbf{u}_1 \\ \mathbf{u}_2 \\ p \end{pmatrix} = \begin{pmatrix} -\mathrm{e}^x(y\cos(y)+\sin(y)) \\ \mathrm{e}^x y\sin(y) \\ 2\mathrm{e}^x\sin(y) - (2(1-\mathrm{e})(\cos(1)-1))/3 \end{pmatrix}.$$

In Figure 2(a) we show the mesh generated using the proposed a posteriori error indicator after 10 adaptive refinement steps. Here, we see that while the mesh has been largely uniformly refined throughout the entire computational domain, additional refinement has been performed where the gradient/curvature of the analytical solution is relativity large; cf. Figures 2(b), (c) and (d), where we plot the isolines of the

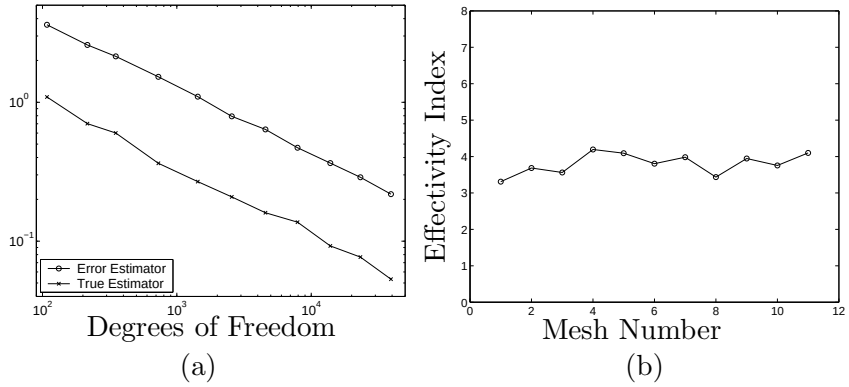

Figure 3. Example 1. (a) Comparison of the actual and estimated energy norm of the error with respect to the number of degrees of freedom; (b) Effectivity Indices.

numerical approximation to $\mathbf{u}_1$, $\mathbf{u}_2$ and p, respectively, computed on this mesh.

Finally, in Figure 3(a) we present a comparison of the actual and estimated energy norm of the error versus the number of degrees of freedom in the finite element space $\mathbf{V}_h \times Q_h$, on the sequence of meshes generated by our adaptive algorithm. Here, we observe that the error bound over-estimates the true error by a consistent factor; indeed, from Figure 3(b), we see that the computed effectivity indices lie in the range between 3–4.

5.2. Example 2

In this section, we consider the example of the singular solution to (1) proposed in Verfürth [23, p. 113]. To this end, we again let Ω be the L–shaped domain shown in Figure 1, and select $\mathbf{f} = \mathbf{0}$ and $\nu = 1$. Then, writing (r, φ) to denote the system of polar coordinates, we impose an appropriate inhomogeneous boundary condition for $\mathbf{u}$ so that

$$\begin{aligned} \mathbf{u}(r,\varphi) &= r^{\lambda} \begin{pmatrix} (1+\lambda)\sin(\varphi)\Psi(\varphi) + \cos(\varphi)\Psi'(\varphi) \\ \sin(\varphi)\Psi'(\varphi) - (1+\lambda)\cos(\varphi)\Psi(\varphi) \end{pmatrix}, \\ p &= -r^{\lambda-1}[(1+\lambda)^2\Psi'(\varphi) + \Psi'''(\varphi)]/(1-\lambda), \end{aligned}$$

where

$$\begin{aligned} \Psi(\varphi) &= \sin((1+\lambda)\varphi)\cos(\lambda\omega)/(1+\lambda) - \cos((1+\lambda)\varphi) \\ &\quad - \sin((1-\lambda)\varphi)\cos(\lambda\omega)/(1-\lambda) + \cos((1-\lambda)\varphi), \\ \omega &= \frac{3\pi}{2}. \end{aligned}$$

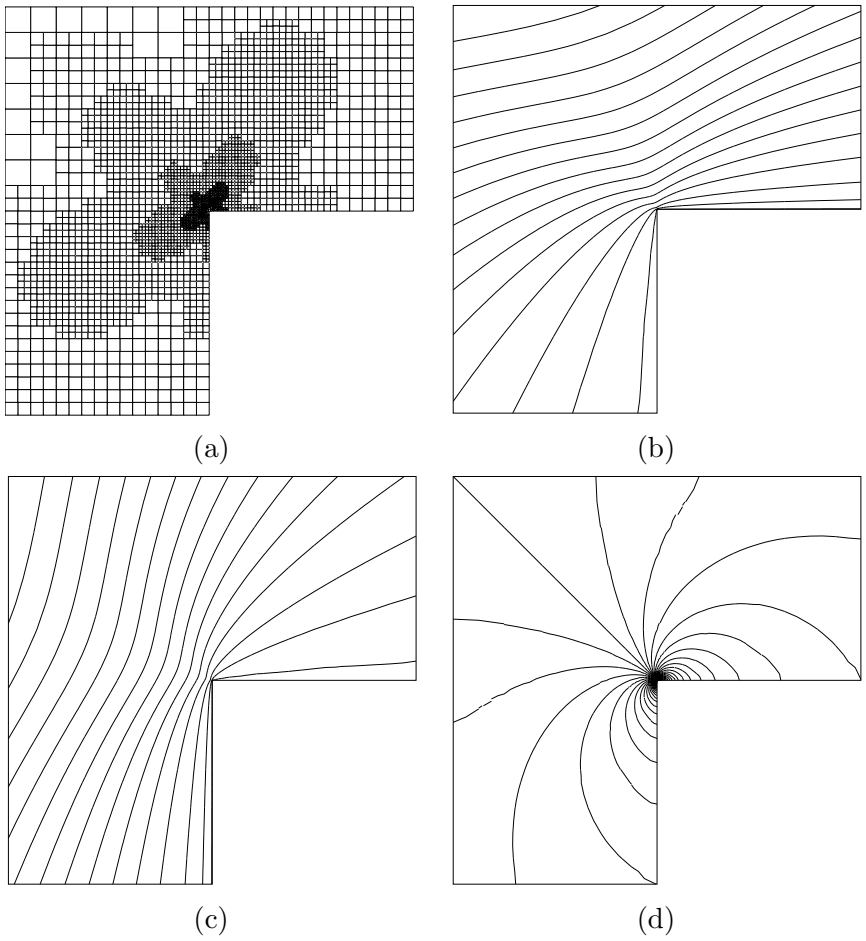

Figure 4. Example 2. (a) Computational mesh with 3009 elements, after 8 adaptive refinements. Numerical approximation to: (b) $\mathbf{u}_1$; (c) $\mathbf{u}_2$; (d) p.

The exponent λ is the smallest positive solution of

$$\sin(\lambda\omega) + \lambda \sin(\omega) = 0;$$

thereby, $\lambda \approx 0.54448373678246$.

We emphasize that $(\mathbf{u}, p)$ is analytic in $\overline{\Omega} \setminus \{\mathbf{0}\}$, but both $\nabla \mathbf{u}$ and p are singular at the origin; indeed, here $\mathbf{u} \notin H^2(\Omega)^2$ and $p \notin H^1(\Omega)$. This example reflects the typical (singular) behavior that solutions of the two-dimensional Stokes problem exhibit in the vicinity of reentrant corners in the computational domain.

In Figure 4(a) we show the mesh generated using the local error indicators η_K after 8 adaptive refinement steps. Here, we see that the

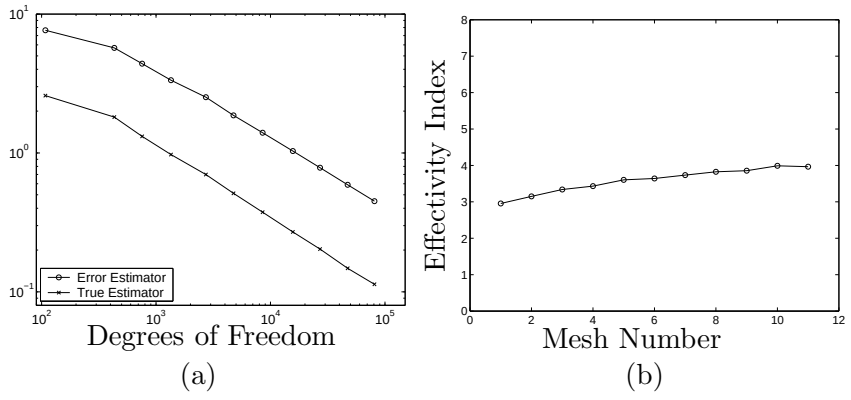

Figure 5. Example 2. (a) Comparison of the actual and estimated energy norm of the error with respect to the number of degrees of freedom; (b) Effectivity Indices.

mesh has been largely refined in the vicinity of the re-entrant corner located at the origin, as well as in the region adjacent to this singular point; indeed, away from the origin, we see that the mesh is (almost) symmetric about the line $y = -x$. The isolines of the numerical approximation $(\mathbf{u}_h, p_h)$ computed on this mesh are shown in Figures 4(b), (c) and (d), respectively. Finally, Figure 5 shows the history of the actual and estimated energy norm of the error on each of the meshes generated by our adaptive algorithm, together with their corresponding effectivity indices. As in the previous example, we observe that the a posteriori bound over-estimates the true error by a consistent factor between 3–4, though here we do see that for this non-smooth example, the effectivity indices do grow very slightly as the mesh is refined; asymptotically they seem to be tending towards a constant value of approximately 4.

6. Concluding Remarks

In this paper, we have derived a residual–based energy norm a posteriori error bound for mixed DG approximations of the Stokes equations. The analysis is based on employing a non-consistent reformulation of the DG scheme, together with a decomposition result for the underlying discontinuous space. Numerical experiments presented in this article clearly demonstrate that the proposed a posteriori estimator converges to zero at the same asymptotic rate as the energy norm of the actual error on sequences of adaptively refined meshes. Future work will be devoted to the extension of our analysis to *hp*-adaptive discontinuous Galerkin approximations of more complicated incompressible flow models.

References

1. D.N. Arnold, F. Brezzi, B. Cockburn, and L.D. Marini. Unified analysis of discontinuous Galerkin methods for elliptic problems. *SIAM J. Numer. Anal.*, 39:1749–1779, 2001.
2. G.A. Baker, W.N. Jureidini, and O.A. Karakashian. Piecewise solenoidal vector fields and the Stokes problem. *SIAM J. Numer. Anal.*, 27:1466–1485, 1990.
3. R. Becker, P. Hansbo, and M.G. Larson. Energy norm a posteriori error estimation for discontinuous Galerkin methods. *Comput. Methods Appl. Mech. Engrg.*, 192:723–733, 2003.
4. R. Becker, P. Hansbo, and R. Stenberg. A finite element method for domain decomposition with non-matching grids. *Math. Model. Anal. Numer.*, 37:209–225, 2003.
5. F. Brezzi and M. Fortin. Mixed and hybrid finite element methods. In *Springer Series in Computational Mathematics*, volume 15. Springer–Verlag, New York, 1991.
6. B. Cockburn, G. Kanschat, and D. Schötzau. The local discontinuous Galerkin method for the Oseen equations. *Math. Comp.*, 73:569–593, 2004.
7. B. Cockburn, G. Kanschat, D. Schötzau, and C. Schwab. Local discontinuous Galerkin methods for the Stokes system. *SIAM J. Numer. Anal.*, 40:319–343, 2002.
8. M. Dauge. Stationary Stokes and Navier–Stokes systems on two- or three-dimensional domains with corners. Part I: Linearized equations. *SIAM J. Math. Anal.*, 20(1):74–97, 1989.
9. K. Eriksson, D. Estep, P. Hansbo, and C. Johnson. Introduction to adaptive methods for differential equations. In A. Iserles, editor, *Acta Numerica*, pages 105–158. Cambridge University Press, 1995.
10. V. Girault and P.A. Raviart. *Finite element methods for Navier–Stokes equations*. Springer–Verlag, New York, 1986.
11. V. Girault, B. Rivière, and M.F. Wheeler. A discontinuous Galerkin method with non-overlapping domain decomposition for the Stokes and Navier-Stokes problems. Technical Report 02-08, TICAM, UT Austin, 2002. In press in Math. Comp.
12. P. Hansbo and M.G. Larson. Discontinuous finite element methods for incompressible and nearly incompressible elasticity by use of Nitsche's method. *Comput. Methods Appl. Mech. Engrg.*, 191:1895–1908, 2002.
13. P. Houston, I. Perugia, and D. Schötzau. Mixed discontinuous Galerkin approximation of the Maxwell operator. Technical Report 02-16, Department of Mathematics, University of Basel, 2002. In press in SIAM J. Numer. Anal.
14. P. Houston, I. Perugia, and D. Schötzau. Energy norm a posteriori error estimation for mixed discontinuous Galerkin approximations of the Maxwell operator. Technical Report 2003-17, Department of Mathematics and Computer Science, University of Leicester, 2003.
15. G. Kanschat and R. Rannacher. Local error analysis of the interior penalty discontinuous Galerkin method for second order elliptic problems. *J. Numer. Math.*, 10:249–274, 2002.
16. O.A. Karakashian and W.N. Jureidini. A nonconforming finite element method for the stationary Navier-Stokes equations. *SIAM J. Numer. Anal.*, 35:93–120, 1998.
17. O.A. Karakashian and F. Pascal. A posteriori error estimation for a discontinuous Galerkin approximation of second order elliptic problems. Technical

report, University of Tennessee, Department of Mathematics, 2003. URL: `http://www.math.utk.edu/~ ohannes/papers.html`.
18. I. Perugia and D. Schötzau. An *hp*-analysis of the local discontinuous Galerkin method for diffusion problems. *J. Sci. Comput.*, 17:561–571, 2002.
19. B. Rivière and M.F. Wheeler. A posteriori error estimates for a discontinous Galerkin method applied to elliptic problems. *Comput. Math. Appl.*, 46:141–163, 2003.
20. D. Schötzau, C. Schwab, and A. Toselli. Mixed *hp*-DGFEM for incompressible flows. *SIAM J. Numer. Anal.*, 40:2171–2194, 2003.
21. D. Schötzau and T.P. Wihler. Exponential convergence of mixed *hp*-DGFEM for Stokes flow in polygons. *Numer. Math.*, 96:339–361, 2003.
22. A. Toselli. *hp*-Discontinuous Galerkin approximations for the Stokes problem. *Math. Models Methods Appl. Sci.*, 12:1565–1616, 2002.
23. R. Verfürth. *A review of a posteriori error estimation and adaptive mesh-refinement techniques*. Teubner, Stuttgart, 1996.
24. T.P. Wihler, P. Frauenfelder, and C. Schwab. Exponential convergence of the *hp*-DGFEM for diffusion problems. *Comput. Math. Appl.*, 46:183–205, 2003.